

International airport emissions and their impact on local air quality: Chemical speciation of ambient aerosols at Madrid-Barajas Airport during AVIATOR Campaign

Saleh Alzahrani¹, Doğuşhan Kılıç^{1,2}, Michael Flynn¹, Paul I. Williams^{1,2} and James Allan^{1,2}

¹Department of Earth and Environmental Sciences, University of Manchester, Manchester, UK

²National Centre for Atmospheric Science, University of Manchester, Manchester, UK

Correspondence to: Saleh Alzahrani (Saleh.alzahrani@manchester.ac.uk)

Abstract. Madrid-Barajas International Airport (MAD), is the fourth-busiest airport in Europe. The aerosol chemical composition and the concentrations of other key pollutants were measured at the airport perimeter during October 2021, to assess the impact of airport emissions on local air quality. A high-fidelity ambient instrumentation system was deployed at Madrid Airport to measure: concentrations of organic aerosols (with their composition), black carbon (*e*BC), carbon dioxide (CO₂), carbon monoxide (CO), nitrogen dioxide (NO_x), sulphur dioxide (SO₂), particulate matter (PM_{2.5}, PM₁₀), total hydrocarbon (THC), and total particle number. The average concentration of *e*BC, NO_x, SO₂, PM_{2.5}, PM₁₀, CO and THC at the airport for the entire campaign were, 1.07 (µg/m³), 22.7 (µg/m³), 4.10 (µg/m³), 9.35 (µg/m³), 16.43 (µg/m³), 0.23 (mg/m³) and 2.30 (mg/m³) respectively. The source apportionment analysis of the non-refractory organic aerosol (OA) using positive matrix factorisation (PMF) allowed us to discriminate between different sources of pollution, namely: Less Oxidised Oxygenated Organic Aerosol (LO-OOA), Alkane Organic Aerosol (AlkOA), and More Oxidised Oxygenated Organic Aerosol (MO-OOA). The results showed that LO-OOA and MO-OOA accounts for more than 80% of the total organic particle mass measured near runway. Trace gases correlate better with AlkOA factor than LO-OOA and MO-OOA indicating that AlkOA is mainly related to the primary combustion emissions. Bivariate polar plots were used for the pollutant source identification. Significantly higher concentrations of the obtained factors were observed at low wind speeds (< 3m/s) from the southwest, where two of runways, and all terminals are located. Higher SO₂/NO_x and CO/*e*BC ratios were observed when the winds originating from the northeast, where the two northern runways are located. These elevated ratios are attributed to the aircraft activity being the major source in the northeast area.

1. Introduction

Several studies have linked particulate matter (PM) to a range of harmful health effects, including respiratory and cardiovascular ailments (Boldo et al., 2006; Li et al., 2003a; Pope and Dockery, 2006; Schwarze et al. et al., 2006). In recent years, a number of researchers have found an association between aviation emissions and potential adverse human health impacts. These emissions can lead to immune system malfunction, various pathologies, the development of cancer, and premature death. Hence, it is increasingly recognised as a serious, worldwide public health concern (Yim et al., 2013; He et al., 2018; Jonsdottir et al., 2019). Airports contribute to primary and secondary inhalable and fine particulate matter (PM₁₀ and PM_{2.5}, with aerodynamic diameters of <10 µm and <2.5 µm, respectively), making them key determinants of urban air quality and a significant concern for local air quality management.

A few studies have reported that air pollutants emitted from large airports can play a vital role in worsening the regional air quality (Rissman et al., 2013; Hudda and Fruin, 2016). Hu et al., (2009) and Westerdahl et al., (2008) measured high ambient PM concentrations downwind of Los Angeles International Airport (LAX) and Santa Monica Airport (SMA) in California. A decline in the ambient air quality was observed up to 18 km downwind from international airports due to an increase in particle number concentrations linked to gas turbine-emitted PM (Hudda et al., 2014; Hudda and Fruin, 2016). To date, several questions still remain to be answered regarding the chemical composition of aircraft plumes, and the health risks associated with the exposure to the pollutants originating from airports in neighbouring communities. Responding to the growing concern about the risk of exposure to airport pollutants, studies have been conducted to gain a better understanding of airport emissions and their possible effects on local and regional air quality. Thus far, aircraft engines are considered to be one of the major sources of both gaseous and particulate pollutants at the airport (Masiol and Harrison, 2014). Various campaigns have reported both physical and chemical properties of particulate and gaseous emissions (Kinsey,

58 2009; Kinsey et al., 2010, 2011; Mazaheri et al., 2011; Hudda et al., 2016). Aviation fuel Jet A1 is the most
59 common type of fuel that is used in civil aviation. It's a complex mixture of aliphatic hydrocarbons and aromatic
60 compounds, characterized by a mean C/H ratio of ~ 0.52 (with an average empirical molecular formula of $C_{12}H_{23}$)
61 (Lee et al., 2010). The mass fraction of paraffins in jet fuel is over or equal to 75%, while the aromatic content is
62 less than or equal to 25% (Liu et al., 2013). Although there are several fuel combustion sources at airports,
63 including aircraft operation and diesel ground transport, the combustion of the aviation fuel increases maximum
64 particle counts in the 10 - 20 nm range based on the particle size distribution analysis (Zhu et al., 2011). Other
65 sources of airport-related PM emissions also contribute to local air pollution. Approximately 38% of PM_{10} , with
66 a mean level of $48 \mu\text{g}/\text{m}^3$ at airports, can periodically originate from the construction activities related to terminal
67 maintenance and expansion (Amato et al., 2010). Particles emitted by commercial aircraft can be divided into two
68 main groups: non-volatile and volatile PM. Non-volatile PM (nvPM) is usually formed during the (incomplete)
69 combustion process and then emitted from the aircraft combustion chamber. It consists mostly of carbonaceous
70 substances such as soot, dust, and trace metals (Yu et al., 2019). nvPM has the physical property of being resistant
71 to high temperatures and pressure. On the other hand, volatile PM is formed through gas to particle conversion
72 process, primarily by sulphur and organic compounds, which exist in the exhaust gas downstream of the engine
73 after emission. Sulphuric compounds are formed as a result of sulphur in fuel, whereas organic particles are formed
74 as combustion products, and from fuel and oil vapours (ICAO, 2016; Smith et al., 2022). Aircraft and ground unit
75 emissions have been documented in prior research (Masiol and Harrison, 2014), yet there is still a gap in
76 knowledge about airport-related PM emissions in terms of (i) apportioning PM to individual sources at airports,
77 (ii) specifying their chemical composition, and (iii) the wider impacts of PM on local communities. This study
78 aimed to obtain data to address these research gaps by providing further in-depth information on particle
79 composition measurements and key pollutants observed within an airport environment. It characterises organic
80 volatile PM emissions to assess the effect of aviation emissions on the local air quality. As part of the AVIATOR
81 Project (Assessing aViation emission Impact on local Air quality at airports: TOwards Regulation), ambient
82 measurements were conducted at Madrid-Barajas Airport to monitor the chemical properties of sub-micron
83 particles near the runways. Source apportionment analysis was performed based on the particle data collected via
84 high resolution mass spectrometry and this analysis allowed us to discriminate between different sources of air
85 pollution at the airport microenvironment. These findings will serve as the foundation for additional
86 comprehensive research, such as toxicological and health effect studies of PM originating from aviation activities.
87

88 2. Methods

89 2.1. Description of the sampling location

90
91 Adolfo Suárez Madrid-Barajas Airport is the main international airport in Spain, located within the municipal
92 limits of Madrid, 13 km northeast of Madrid's city centre. It is the fourth-busiest airport in Europe based on
93 passenger volume (Eurostat Database, 2021). In 2019, 62 million travellers used Madrid-Barajas and nearly half
94 a million aircraft movements have been recorded, making it the largest and busiest airport in the country. In 2021,
95 nearly one-third of the previous number travelled through Madrid Airport because of the COVID-19 pandemic.
96 The airport has five passenger terminals named T1, T2, T3, T4, and T4S. Barajas Airport also has four runways:
97 two on the north-south axis, parallel to each other (18L/36R and 18R/36L), and two on the northwest-southeast
98 axis (14L/32R and 14R/32L). The runways enable simultaneous takeoffs and landings at the airport, allowing 120
99 operations per hour (one takeoff or landing every 30 seconds). The sampling location was chosen in collaboration
100 with AENA, the owner and operator of the Barajas Airport, to facilitate the provision of power and access for
101 servicing. Focusing on the temporal and spatial monitoring of the key pollutants, the site was positioned between
102 runways 36L and 36R to sample the airport emissions from an optimal sampling point for aviation activities
103 (Fig.1). The distance from sampling location to the runways 18L/36R, 18R/36L, 14L/32R and 14R/32L are 680
104 m, 620 m, 3.2 km, and 4.1 km respectively. Furthermore, the distance between sampling location and adjacent
105 terminals T1, T2, T3 is approximately 5 km whereas 3 km and 1.5 km to the terminals T4 and TS4 respectively.
106 The nearest highway is located around 2.6 km away from the sampling location.
107

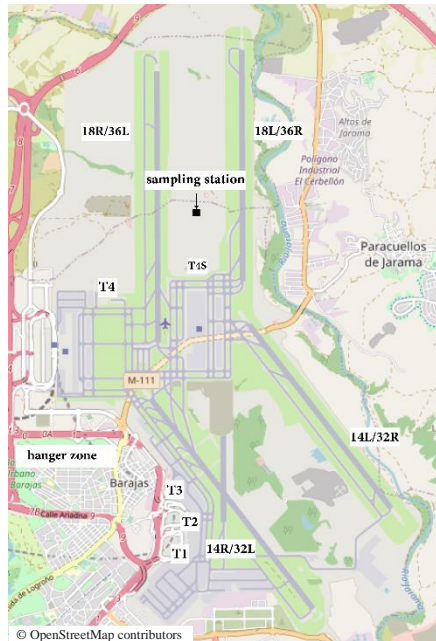


Figure 1. Locations of runways, terminals, and sampling site at Adolfo Suárez Madrid-Barajas Airport. Measurements were performed between October 8, 2021 and October 23, 2021. (Adapted from: <https://www.openstreetmap.org>)

2.2. Sampling and instrumentation

The autumn campaign of AVIATOR took place in October 2021. Sampling was conducted continuously, starting at 12:00 pm on October 8, 2021 and ending at 20:00 pm on October 23, 2021. An ambient instrumentation system with specific reference to PM was deployed at Madrid Airport to better characterise air quality at the airport microenvironment. The measurement equipment of the system includes an Aerodyne High-Resolution Time-of-Flight Aerosol Mass Spectrometer (AMS) for the chemical speciation of the particles. AMS measures concentration and chemical composition of non-refractory aerosols online. AMS provided high-resolution measurements of primary and secondary organic aerosol and inorganic aerosol including sulphates, nitrates, and ammonium, from approximately 60 nm to 600 nm with 100 % transmission, extending to smaller and larger sizes with reduced transmission (Canagaratna et al., 2007). An aerodynamic lens is used to draw aerosols into a vacuum chamber. Particles are focused into a narrow beam and accelerated to a velocity inversely related to their vacuum aerodynamic diameter. The particles impact on a tungsten surface, heated to 600 °C, which causes them to flash vaporise. A 70-eV electron is used to ionize the vapours before they are analysed by mass spectrometry. During the measurement period, AMS was sampling with 1µm cut-off inlet and at 30 s time resolution. In addition to standard AMS flow, baseline and single ion calibrations every second day, an ammonium nitrate solution was atomised to calibrate the AMS (for size-dependent ionisation efficiency). The analysis of the chemical characteristics of aircraft PM using an AMS have been described elsewhere in detail (Yu et al., 2010; Anderson et al., 2011; Smith et al., 2022). Equivalent black carbon mass concentration (*e*BC) based on aerosol optical absorption was monitored using the Multi-Angle Absorption Photometer (MAAP) during this campaign. The MAAP operates at 670nm wavelength, has a 10s-time response with a flow rate of 8 litre/min, for unattended long-term monitoring of carbonaceous particulate emissions from combustion sources (Petzold and Schonlinner, 2004). MAAP has been used for the monitoring of black carbon emission from aviation (Herndon et al., 2008; Timko et al., 2014). The instrument was set up to measure average *e*BC concentrations with one-minute intervals. By using a condensation particle counter (CPC), TSI model 3750 ($D_{50} \approx 7\text{nm}$), total particle number concentration was measured real-time to capture temporal variability in particle number concentrations with a measurement range of up to 100,000 particles/cm³ and a time resolution of one second. Ambient CO₂ concentration near runways were also measured by a LI-COR CO₂ Trace Gas Analysers at 1-sec intervals. In addition, meteorological parameters (temperature, pressure, relative humidity, wind speed, and direction) were measured at the site with the instrumentation system. The system was co-located with AENA (REDAIR) fixed monitoring site to provide additional spatially resolved data. The REDAIR station monitors the concentration of sulphur dioxide (SO₂), nitrogen dioxide (NO_x), carbon monoxide (CO), ozone (O₃), suspended particles PM (including PM_{2.5}, PM₁₀), and total hydrocarbon (THC) with a time resolution of 30 minutes.

148
149
150
151
152
153
154
155
156
157
158
159
160
161
162
163
164
165
166
167
168
169
170
171
172
173
174
175
176
177
178
179
180
181
182
183
184
185
186

2.3. Data analysis

AMS was operating in Mass Spectrum (MS) mode to identify the chemical species present in the aerosol ensemble and quantify the overall mass loading. AMS data were analysed using the data analysis toolkit TOF-AMS SQUIRREL v1.65B, operated within Igor Pro (WaveMetrics, Inc.). The Source Finder (SoFi) is a software package designed to analyse multivariate data using state-of-the-art source apportionment techniques to understand the sources of various pollutants (Canonaco et al., 2013). SoFi, running under IGOR 6.37, was used to deconvolve organic aerosol emissions via the Positive Matrix Factorization (PMF) model. The PMF model, implemented through the multilinear engine version 2 (ME-2) factorisation tool, was used to determine the number of factors (sources). ME-2, a multivariate solver, employs the same mathematical/statistical method as PMF to evaluate solutions (Paatero, 1999). ME-2 equations are designed for analysing and calculating the relative contributions of various source pollutants by measuring their concentration at receptor locations (Paatero and Tapper, 1994). The PMF model processes many variables and categorises them into two types (i) source types, which can be determined based on the chemical composition of the pollutants, and (ii) source contributions, used to quantify the amount of contribution from each source to a sample. PMF inputs were restricted to only non-negative concentrations since no sample can have a negative source contribution. A step-by-step approach was employed to select the number of solutions (factors). The method described by Reyes et al. (2016) and Smith et al. (2022) was used to determine the optimal solution. This approach began initially with a two-factor model and then incrementally increased to a maximum of five factors. PMF analysis was performed with seed runs and varying FPEAK values (ranging from -1 to 1 with steps of 0.1) to better differentiate organic aerosol sources. Seed runs and FPEAK are rotational techniques in the ME-2 tool, and they represent one of the unconstrained PMF run approaches used for the exploration of the solution space. During the analysis, it was noted that factor four consistently correlates with factor five, exhibiting identical time series and similarities in mass spectra. This difficulty in separation has previously been observed in the case of well-mixed pollutants, attributed to low temperatures and wind speeds (Reyes et al., 2018). Greater stability was achieved when analysing 3-factor solutions with varying FPEAK values. During the analysis, seed runs and PMF with FPEAK solutions showed no significant variation in the normalised scaled residuals parameter (Q / Q_{exp}), with values close to 1. This is reasonable given that PMF determines the solution by minimising this value (Reyes et al., 2016). The factorisation strategy was entirely successful in separating three different sources, each with distinct mass spectra and differing time series. Consequently, 3-factor solutions emerged as the optimal number of sources, demonstrating the best performance with the lowest residuals and Q/Q_{exp} values close to 1. Furthermore, the obtained solution exhibited the most favorable results, characterized by distinct diurnal trends and dissimilarities in time series and mass-to-charge ratios among the factors.

3. Results and Discussion

3.1 Variations of organic, inorganic, and oil emissions

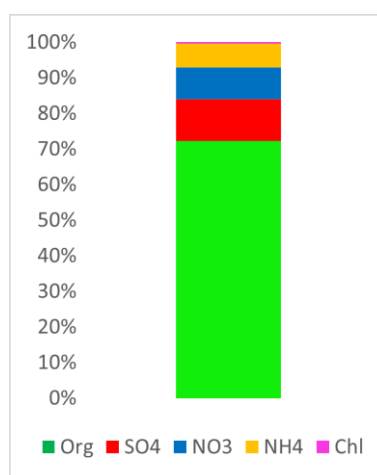
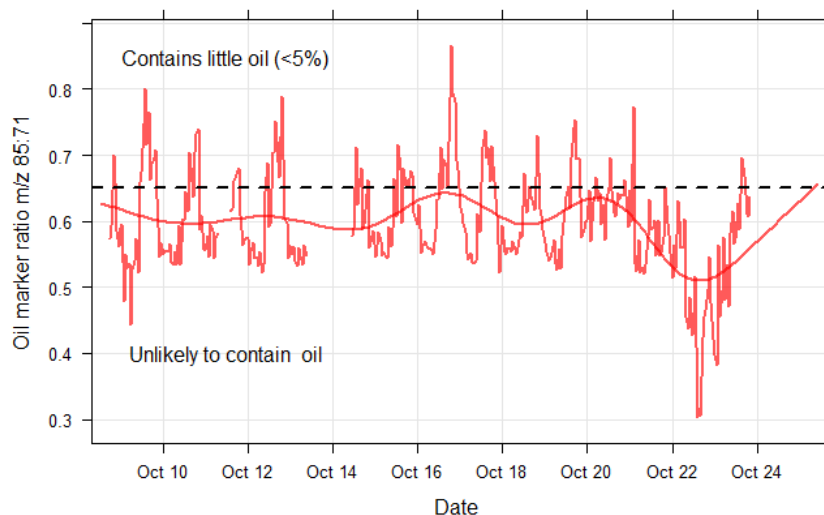


Figure 2. The bar chart shows aerosol fractions where organic and sulphate species account for more than 80% of the total aerosol mass.

187
188
189
190
191
192
193
194

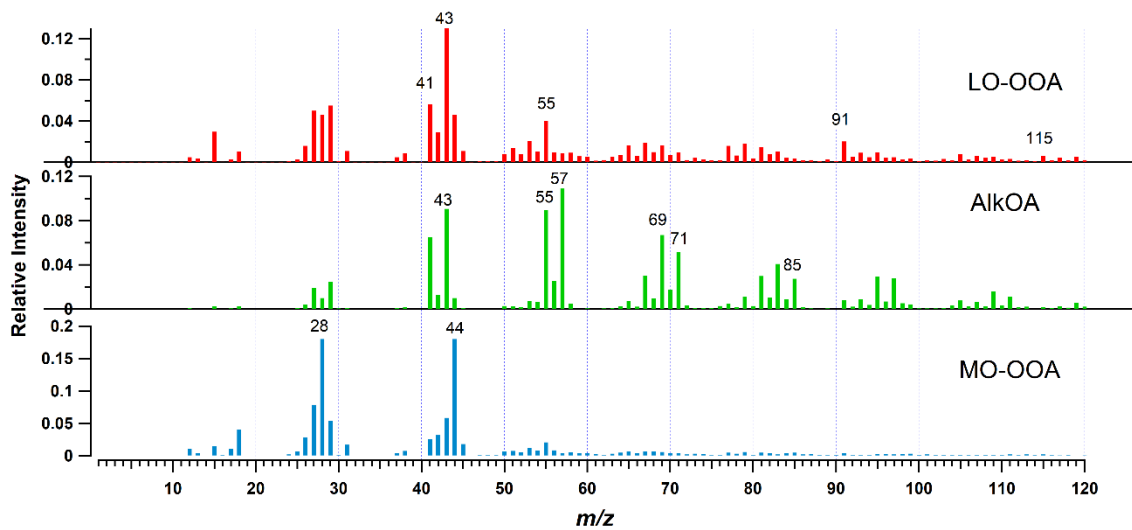
The average mass concentration of organic and inorganic aerosols during the entire campaign was $9.6 \mu\text{g}/\text{m}^3$. The bar chart in Fig. 2 shows aerosol fractions, with organic species accounting for more than 70% of the total aerosols. This is significantly higher than the nearest component, sulphate, which accounted for 15%. It should also be

195 noted that the nitrate and sulphate species measured by AMS could potentially contain an organic fraction. The
 196 PMF analysis in this paper primarily focuses on the composition of the organic mass concentration, which is
 197 discussed in further detail in Section 3.2. Previous studies have shown that lubrication oil has been detected in
 198 ambient air near runways, and it may further add to the total organic PM emissions due to aircraft engine
 199 operations (Timko et al., 2010b; Yu et al., 2010; Fushimi et al., 2019; Ungeheuer et al., 2022). Aircraft plume
 200 measurements indicated that oil was found to contribute 5% to 100% (Yu et al., 2012). The m/z 85 signal is a
 201 well-known oil marker in the AMS mass spectrum, attributed to synthetic esters ($C_5H_9O^+$) (Timko et al., 2014).
 202 Ratio of m/z 85:71 is used as a marker for oil (Fig. 3). The value of 0.66 was used as a benchmark for oil
 203 contribution (Yu et al., 2012). Values below 0.66 indicate oil-free organic PM, while values above 0.66 suggest
 204 the presence of lubrication oil. However, based on the AMS measurements during AVIATOR autumn campaign,
 205 lubrication oil accounted only up to 5% of the total aerosol mass, which is significantly less compared to the
 206 measurements of Yu et al. (2012). There are three probable explanations on the deficiency of AMS to detect oil
 207 precursors: (i) the oil particles are too small in diameter for AMS to detect, (ii) complete pyrolysis of the oil in
 208 the engine combustion zone forming carbon monoxide (CO) and carbon dioxide (CO₂) (Smith et al., 2022) or
 209 (iii) oil particles contribute to an insignificant amount (by mass) to the organic mass in engine exhaust and
 210 therefore are not detected. Additional factors that could potentially impact the minimal presence of oil lubrication
 211 in this analysis might involve the overall mass loading of aerosols, the influence of urban aerosol emissions, or
 212 the proximity of the sampling point to the nearest runways. Additional information on how the lubrication oil, as
 213 measured by AMS, varies with wind speed and direction is provided in the supplementary material (Fig.S4).
 214 During the AVIATOR autumn campaign, measuring oil was challenging due to the prevalent urban background.
 215 A "little oil" region was identified at low to moderate wind speeds (2~5 m/s) originating from the southwest,
 216 encompassing terminal buildings (T1, T2, T3, T4, and TS4), two runways (14R/32L and 18R/36L), and a hangar
 217 zone. In contrast, a region "unlikely to contain oil" was noted when winds came from the northeast of the airport,
 218 near runways 18L/36R, with relatively higher wind speeds (above 5 m/s). Furthermore, Fig.S5 displays the daily
 219 ratio of m/z 85:71 throughout the sampling period, pinpointing Sunday, October 16th, as the only day when the
 220 oil marker surpassed 0.66. On other days, the ratio of m/z 85:71 suggested a minimal likelihood of oil presence.
 221 An hourly analysis within Fig.S5 reveals that the oil marker exceeded 0.66 only at 20:00, aligning with the evening
 222 peak in PM_{2.5} concentrations Fig.S3. This suggests a significant influence of urban background aerosols on the
 223 lubrication oil measurements. Since PMF analysis is based on the organic masses measured via AMS, lubrication
 224 oil is not identified as a determinant and there is no oil organic mass profile reported in previous studies and here
 225 (Ulbrich et al., 2009). PMF has been proven inefficient at detecting such levels (Ulbrich et al., 2009), therefore,
 226 oil contribution to the organic mass may be under-represented in this study.



227
 228 **Figure 3. Temporal variability of lubrication oil fraction in total aerosol mass obtained from AMS measurements.**
 229 **The ratio of m/z 85/71 was used as the mass marker to identify lubrication oil. A smooth red line is fitted to the data,**
 230 **while the dashed black line represents the value of 0.66, assumed for oil-free organic PM emitted from aircraft**
 231 **engines. The analysis showed that no oil or very little (<5%) oil fraction was detected during the measurement period.**
 232
 233
 234
 235
 236
 237

238 **3.2 PMF Analysis**
 239



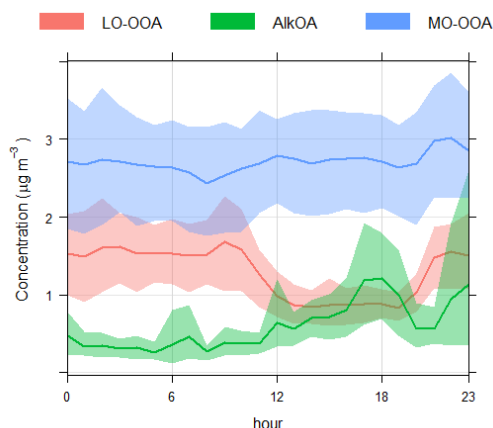
240
 241
 242 **Figure 4. The mass spectral fingerprint of the three factors from the PMF solutions. Less Oxidised Oxygenated**
 243 **Organic Aerosol (LO-OOA), Alkane Organic Aerosol (AlkOA), and More Oxidised Oxygenated Organic Aerosol**
 244 **(MO-OOA), which can be indicative of secondary aerosols. Selected mass markers with a relative intensity higher**
 245 **than 0.01 are numbered.**
 246

247
 248 The PMF analysis in this study aims to provide relative contribution of the sources of aerosols near runway. In
 249 addition to determining the diurnal pattern of the obtained factors during the autumn campaign, PMF solutions
 250 were used to investigate how meteorology affects airborne particulate pollution. During AVIATOR autumn
 251 campaign at Madrid-Barajas International Airport three sources were identified via PMF (Fig. 4 shows the results
 252 of the PMF analysis, the mass spectral fingerprint). The first factor in Fig. 4, LO-OOA, stands for Less Oxidised
 253 Oxygenated Organic Aerosol. It is a type of secondary organic aerosol (SOA) characterized by its low degree of
 254 oxidation. LO-OOA are formed in the atmosphere through the oxidation of volatile organic compounds (VOCs),
 255 which can originate from a variety of anthropogenic sources. In this analysis LO-OOA shows the presence of an
 256 aromatic marker at m/z 115, a marker used for identifying indene (C_9H_8) ion in previous studies focusing on
 257 aviation emissions (Timko et al., 2014; Smith et al., 2022). LO-OOA is associated with aromatic fragments at m/z
 258 77 ($C_6H_5^+$), and 105 ($C_8H_9^+$). It presents a high relative intensity (0.13) at m/z 43 ($C_3H_7^+$) (characteristic of LO-
 259 OOA) and a lower relative intensity (<0.04) at m/z 91, which is related to toluene ion ($C_7H_7^+$) (Timko et al., 2014;
 260 Smith et al., 2022). Ambient temperature plays a crucial role in influencing the LO-OOA factor, displaying
 261 significant diurnal fluctuations. The lowest concentrations of LO-OOA are recorded at midday, coinciding with
 262 the peak in ambient temperatures (Fig. 5). A prior PMF analysis of organic particulate matter from aircraft
 263 emissions revealed a significant aromatic factor within the organic PM, characterized by elevated signals at m/z
 264 77, 91, 105, 115, 128 (Timko et al., 2014). The aromatic factor identified by Timko et al. (2014) was found to
 265 dominate the organic PM emissions from turbojet engines at low-thrust settings. It was associated with the
 266 products of incomplete combustion and exhibited high variability, which varied with engine power settings (the
 267 sum of signals in the factor decreased as engine power increased). Another study by Smith et al. (2022),
 268 investigated the chemical composition of organic aerosols emitted by gas turbines and identified a Semi-Volatile
 269 Oxygenated Organic Aerosol (SV-OOA) factor, which forms through oxidative processes near the engine exit. A
 270 strong correlation ($R = 0.91$) and similarity in mass spectra between the LO-OOA in this study and the SV-OOA
 271 described by Smith et al. (2022) were observed. Owing to the absence of volatility measurements during this
 272 period and the limited time for aging (no more than a few minutes), we consider the LO-OOA factor in our analysis
 273 to be the most accurate estimate available, rather than the SV-OOA as suggested by Smith et al. (2022). The
 274 second factor, identified based on the PMF analysis of Madrid airport sample, is Alkane Organic Aerosol (AlkOA)
 275 factor. It is associated with unburned fuel and emissions from incomplete combustion, exhibiting high relative
 276 intensities at m/z 43, 57, and 85, indicative of decane ($C_{10}H_{22}$), a common alkane in jet fuel. Given that mass
 277 spectral fingerprint of decane is similar to the other aliphatic hydrocarbons (*e.g.*, long-chain alkanes) found in Jet
 278 A1 fuel, as reported by Yu et al. (2012) and Smith et al. (2022). AlkOA factor referred here as a marker to identify
 279 emissions originating from unburnt fuel/incomplete fuel combustion products. Previously, primary aliphatic factor
 280 was found in PMF analysis by Timko et al. (2014) and was characterized by increased signals at masses such as
 281 41/43, 55/57, 69/71, 83/85. Each of these masses correspond to an alkane. The primary aliphatic factor in Timko
 282 et al. (2014) study was strongly correlated with black carbon soot emissions under high-power conditions. The

283 strong association between the primary aliphatic factor and soot emissions suggests they originate from similar
 284 combustion processes. Timko et al. (2014) concluded that the primary aliphatic factor is derived from combustion
 285 related sources and can potentially contain significant amounts of unburnt jet fuel. Additionally, a strong positive
 286 linear correlation was observed between the AlkOA factor identified in this study and the decane factor from
 287 NIST webbook ($R=0.83$) (NIST Mass Spectrometry Data Center, 1990), as well as between the AlkOA factor
 288 determined here and the AlkOA factor reported by Smith et al. (2022) ($R=0.93$). The positive linear correlation
 289 among these three factors suggests they are indicative of similar primary pollutants derived from fuel vapours or
 290 incomplete combustion products associated with jet fuel. Results are consistent with previous findings of another
 291 study (Smith et al., 2022). The third factor, More Oxidised Oxygenated Organic Aerosol (MO-OOA), is a type of
 292 secondary organic aerosol (SOA) that can form from various origins and processes, such as photochemical
 293 processing of aged SOA and the regional-scale transport of chemical reactions. MO-OOA has a spectral
 294 fingerprint that consists of more oxidised ions (compared to LO-OOA and AlkOA), indicating a secondary aerosol
 295 fraction in the sample. MO-OOA is characterized by its notably high relative intensities (>0.18) at m/z 29 (CHO^+)
 296 and 44 (CO_2^+), which serve as markers for its identification (Alfarra et al., 2007). Given that MO-OOA has the
 297 highest $f_{44/43}$ ratio among the three factors, it is expected to be the most oxygenated (in terms of chemical content)
 298 factor. Being more oxidised potentially makes MO-OOA less volatile than LO-OOA (Jimenez et al., 2009;
 299 Smith et al., 2022). MO-OOA in this analysis indicates the formation of aged secondary organic aerosols with no
 300 significant diurnal variation (Fig. 5), often associated with air masses transported from polluted regions. Other
 301 sources may have been included in one or both factor solutions, consequently, this does not rule out the possibility
 302 of their existence.

303
 304
 305
 306

3.3 The temporal distribution of factors and correlation with trace gases



307
 308 **Figure 5. Diurnal pattern of the solved factors from October 8, 2021 to October 23, 2021. The mean diurnal pattern is**
 309 **shown as solid lines, and the shading indicates the 95% confidence interval around the mean.**

310
 311 Average hourly concentrations of the PMF-determined factors were calculated based on the hourly organic aerosol
 312 concentrations throughout the entire campaign to monitor the diurnal variation of the source contributions. The
 313 variation of the AlkOA concentration during the day mostly associated with aircraft emissions (Fig. 5). The
 314 concentration of AlkOA factor is relatively higher in the afternoon compared to the morning and midday. The
 315 pattern of diurnal AlkOA closely resembles that of diurnal flight activities, suggesting that the surge in AlkOA
 316 levels beginning at noon is linked to primary particles released by aircraft. The AlkOA factor shows an increase
 317 between 09:00 and 18:00 and again between 22:00 and 23:00. Based on the mean diurnal pattern with a 95%
 318 confidence interval, the AlkOA factor increases during the 09:00 to 18:00 period, corresponding with peak flight
 319 activity (approximately 71% of total flights). Further details on daily aircraft activities are provided in the
 320 supplementary material (Fig. S2). The increase in AlkOA between 22:00 and 23:00 is not statistically significant
 321 due to high variability (Fig. 5). The increase in AlkOA concentration from 22:00 to 23:00, or the subsequent
 322 decrease from 23:00 to 00:00, falls within the variability range of the 00:00 to 01:00 period. Therefore, a
 323 statistically significant decrease in AlkOA concentration from 23:00 to 00:00 is hardly measurable.
 324 Meteorological factors may contribute to the variability in the diurnal cycle observed during this period.
 325 Additionally, unidentified local source such as airport ground service equipment could potentially explain the
 326 variability observed from 22:00 to 00:00. This source has been previously reported as the main determinant of the
 327 air quality in the vicinity of the airport (Masiol and Harrison, 2014). The LO-OOA factor likely represents fresh
 328 secondary organic aerosols (SOA), demonstrating high variability and sensitivity to ambient temperature

329 fluctuations. The concentration of LO-OOA is at its lowest when daytime temperatures peak. LO-OOA may
330 contain urban contributions and potentially effected by background urban pollution from Madrid. The observed
331 reduction in LO-OOA factor during the afternoon can be attributed to dilution effects resulting from the rise in
332 boundary layer height, along with the potential evaporation of LO-OOA particles due to increased ambient
333 temperatures. This is supported by the variance in background particulate matter concentrations located south of
334 the airport compared to those at the sampling point, approximately 6 km apart, as illustrated in Fig. S3. (Fig. S3)
335 reveals that PM_{2.5} levels at both locations experience significant increases during morning and evening rush hours,
336 with the sampling point consistently showing higher concentrations than the background location. The diurnal
337 pattern of the background location demonstrates a rapid decrease in PM_{2.5} levels in the afternoon, unlike the
338 measurements at the sampling point. Additionally, there is a noticeable lag of about an hour between the peak
339 concentrations at the sampling point and those in the background, suggesting the influence of additional
340 combustion sources of PM_{2.5}, notably aviation-related activities, particularly during periods of increased airport
341 traffic. Unlike other factors, MO-OOA shows no significant diurnal variation, indication the formation of aged
342 secondary organic aerosols, often a result of atmospheric transport (Zhang et al., 2007). Detailed statistics of the
343 obtained factors for the entire campaign are provided in the supplementary material (Table S1). At Madrid-Barajas
344 Airport, AlkOA exhibited moderate correlations with *e*BC, NO_x, SO₂, and CO, as evidenced by the linear
345 correlation coefficients listed in Table 1 (R=0.56, R =0.52, R =0.53, and R =0.52). In contrast, the correlation of
346 these trace gases and both LO-OOA and MO-OOA is lower compared to AlkOA, with R values ranging from 0.2
347 to 0.5, as shown in (Table 1). The slightly higher correlation of AlkOA with BC, NO_x, SO₂ and CO (R > 0.5)
348 relative to LO-OOA and MO-OOA can be attributed to AlkOA being a primary pollutant, emitted directly from
349 the source. Conversely, LO-OOA and MO-OOA are believed to be secondary pollutants, formed through the
350 processes of condensation and coagulation of primary pollutants. In this study, urban contributions are
351 predominantly subject to this processing, as there is insufficient time for significant photochemical oxidation of
352 aviation emissions in such close proximity to the source. Additionally, the diurnal trends of BC, NO_x, SO₂ and
353 CO can be significantly affected by meteorological conditions (*e.g.*, wind speed, temperature) (Carslaw et al.,
354 2006; Reyes et al., 2018). This influence accounts for their moderate correlation with AlkOA, with R values
355 between 0.52 and 0.56, as detailed in Table 1. Similarly, AlkOA could potentially be affected by meteorological
356 conditions. Since AlkOA is measured as part of AMS sub-micron particles, it is expected to behave similarly to
357 *e*BC in the particle phase. Therefore, meteorological conditions likely influence both AlkOA and *e*BC in a similar
358 manner. AlkOA and trace gases were normalised to facilitate comparison of their diurnal patterns, thereby
359 enhancing understanding of their relative contributions and identifying trends among these pollutants.
360 Normalising is accomplished by dividing the concentrations of the pollutants by their average value. Figure 6
361 shows diurnal patterns of AlkOA factor, *e*BC, NO_x, CO, and particle number concentration. The daily trend of
362 *e*BC, NO_x and CO are mostly similar, with very pronounced increases in concentrations during the morning and
363 evening rush hours. The average concentrations were 1.07 µg/m³, 22.7 µg/m³ and 0.23 mg/m³ for *e*BC, NO_x and
364 CO respectively (Table S1). AlkOA gradually increases during the morning, with multiple minor peaks observed
365 in the morning hours. The average concentration of AlkOA is higher at night than during the day. This increase
366 is potentially related to daily aircraft activities. AlkOA began to increase, reaching a maximum during the
367 afternoon rush hour from 12:00-18:00. a second rapid increase occurred around 20:00, potentially caused by an
368 increase in the number of flights at this time (Fig. S2). Early morning AlkOA concentrations are significantly
369 lower compared to those of *e*BC, NO_x and CO. This difference could be attributed to reduced emissions resulting
370 from decreased aircraft activities in early mornings (Fig. S2). The rise in trace gases and *e*BC observed in the
371 early morning hours could originate from various airport operations. Such operations might encompass emissions
372 from auxiliary power units, vehicle traffic, and the use of ground service equipment at the airport (Masiol and
373 Harrison, 2014). The total number concentration exhibited a temporal pattern similar to that of AlkOA from
374 15:00–21:00. Likewise, the temporal profiles of AlkOA and trace gases were similar during the afternoon period
375 (17:00-21:00). This similarity in temporal profiles suggests common source origins, which may be temporally
376 associated with aircraft activity or the influence of background urban pollution.

377

378 **Table 1 Results of linear regression analysis between obtained factors (LO-OOA, AlkOA, and MO-OOA)**
379 **and external tracers. Data from the entire campaign was used to perform the correlation analysis.**

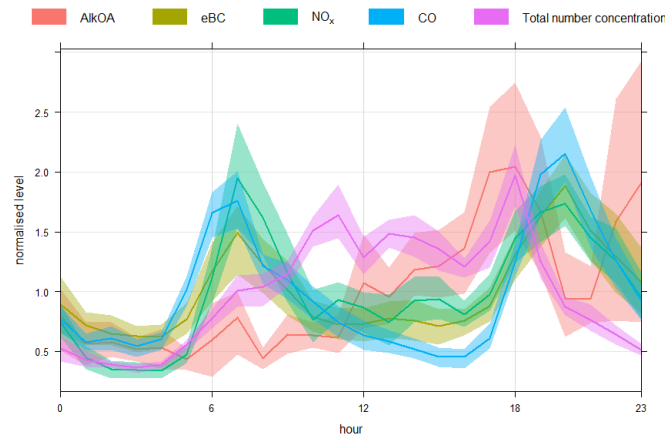
380

	<i>e</i> BC (µg/m ³)	NO _x (µg/m ³)	SO ₂ (µg/m ³)	CO (mg/m ³)	THC (mg/m ³)	PM _{2.5} (µg/m ³)	Tot No. conc (particles/cm ³)	CO ₂ (ppm)
LO-OOA	0.49	0.28	0.21	0.32	0.63	0.36	-0.08	0.24
AlkOA	0.56	0.52	0.53	0.52	0.35	0.66	0.4	0.35
MO-OOA	0.48	0.36	0.26	0.45	0.41	0.55	0.1	0.22

381

382

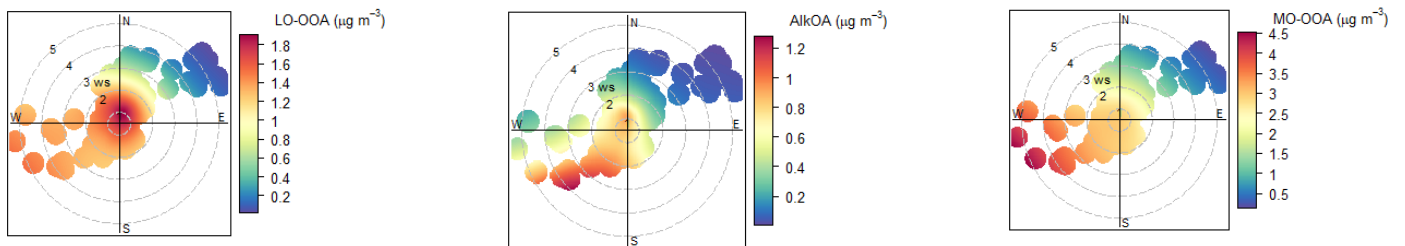
383
384



385
386
387
388
389
390
391

Figure 6. The diurnal cycle of AlkOA compared to eBC, NO_x, CO, and total number concentration. In this plot, the concentrations are normalised with the objective of comparing the patterns of different pollutants using the same scale.

3.4 Spatial analysis



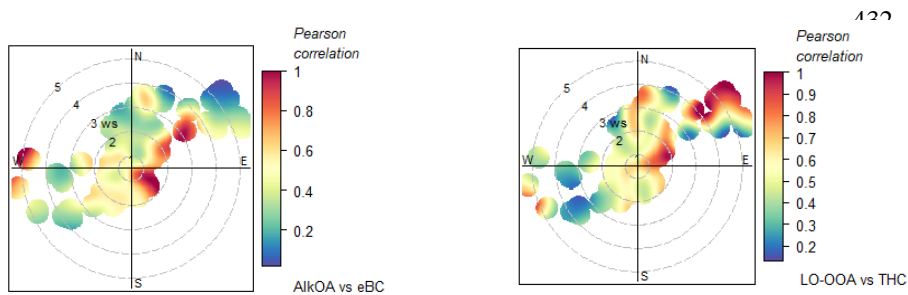
392
393
394
395
396
397

Figure 7. Bivariate polar plots for LO-OOA, AlkOA, and MO-OOA ($\mu\text{g}/\text{m}^3$). The highest concentrations were measured when the winds originated from the west and southwest. Runways 18R/36L and 14R/32L located at western and eastern sides of the measurement station and the hanger zone with terminals T1, T2, T3, T4, and TS4 are located at the south and southwest of the measurement site (Fig. 1).

398
399
400
401
402
403
404
405
406
407
408
409
410
411
412
413
414
415
416
417

Varying sources can be discriminated by means of bivariate polar plots techniques (Carslaw and Ropkins, 2012). Figure 7 illustrates the impact of airport activities on the average concentrations of factors (LO-OOA, AlkOA and MO-OOA) as determined by PMF. The highest concentrations of AlkOA and MO-OOA were observed at low to moderate wind speeds (3~5 m/s) coming from the west and southwest ($R = -0.35$ and $R = -0.42$, respectively), near the terminal buildings (T1, T2, T3, T4 and TS4), two of the runways (14R/32L and 18R/36L), and a nearby hanger zone. The most significant contributions of LO-OOA occur at wind speeds below 2 m/s, with a correlation of $R = -0.45$. At such low wind speeds (< 2 m/s), LO-OOA and MO-OOA are more likely to be mixed and influenced by a nearby source (Crilley et al., 2015; Helin et al., 2018). By contrast, the minimum significant contribution from all factors was observed when the winds originated from the northeast of the airport, accompanied by relatively higher wind speeds (above 4 m/s). Thus, based on the polar plots shown in Fig. 7, emissions from the terminal buildings and hanger zone located at the southwest of the measurement station are the major sources of total organic particle concentrations at the measurement station. The average contributions of LO-OOA, AlkOA, and MO-OOA were 1.63, 0.63, and 2.35 $\mu\text{g}/\text{m}^3$, respectively (Table S1). During the AVIATOR campaign in October 2021, LO-OOA and MO-OOA constituted more than 80% of the total organic mass. Based on the strength of the relationship outlined in Table 1 between derived factors and external tracers, the linear correlations (Pearson correlation) between (i) AlkOA with eBC and (ii) LO-OOA with THC were measured under varying wind speed and directions, as illustrated in (Fig. 8). The relative contributions of the AlkOA and LO-OOA were higher with winds originating from southwest of the airport, compared to when winds carried air parcels to the sampling point from the northeast, as discussed. However, the correlation coefficient for these factors varies significantly, ranging from 0.2 to 0.9, for all samples collected from various directions within the airport perimeter. For instance, AlkOA

418 exhibits a strong linear correlation with *e*BC (Pearson coefficient higher than 0.9) when winds originate from the
 419 west, east, or northeast, as illustrated in Fig. 8. This correlation is attributed to the impact of runways 18L/36R
 420 and 18R/36L, which are situated to the east and west of the measurement site, respectively, as depicted in Fig. 1,
 421 where 90% of aircraft take-offs occur. Both AlkOA and *e*BC are related to jet fuel emissions, as they are directly
 422 emitted by aircraft engines as a result of fuel combustion. *e*BC emissions are a function of engine power settings,
 423 reaching their maximum at full thrust during take-off (Kinsey et al. 2011; Hu et al., 2009). Furthermore, a
 424 significant linear correlation was measured between LO-OOA and THC when dominant winds were north
 425 easterlies (the air parcels move from runways 18L/36R to the sampling station). THC emissions at airports
 426 primarily dependent on the jet engine thrust setting (Anderson et al., 2006; Onasch et al., 2009). When engines
 427 operate at low thrust settings (*e.g.*, during landing, taxiing, idling), combustion is less efficient, leading to the
 428 emission of higher amounts of hydrocarbons. The association between LO-OOA and THC in certain areas of the
 429 airport can be interpreted as indicative of fresh emissions from aircraft in service.
 430
 431

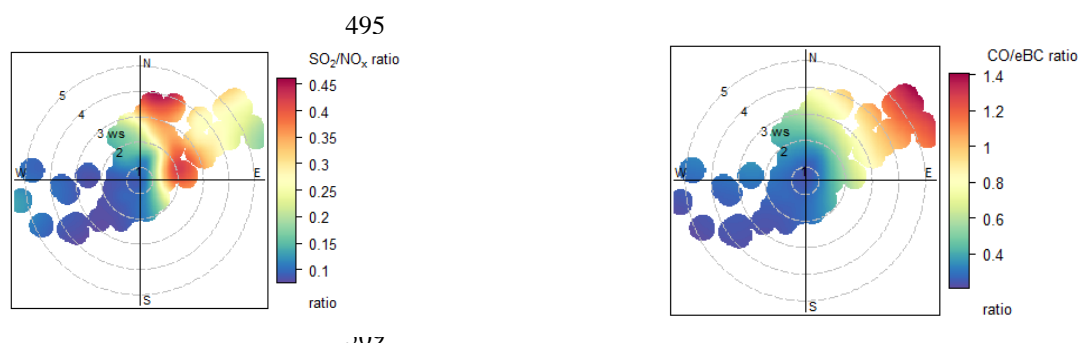


445
 446 **Figure 8. A Pearson correlation analysis using bivariate polar plots (above) shows a significant positive linear**
 447 **correlation between AlkOA with *e*BC and LO-OOA with THC mass concentrations when prevailing winds were**
 448 **northeast. (The location of runways 18L/36R).**
 449

450 NO_x emitted by aircraft can potentially affect air quality up to 2.6 km away from the airport (Carslaw et al., 2006).
 451 However, accurately determining the airport's contribution to local NO_x concentrations presents challenges due
 452 to other predominantly mobile sources of NO_x in urban areas. In this study, the potential contribution of road
 453 traffic surrounding the airport, particularly from the motorways located to the south and southwest, originates
 454 from the same direction as runway 14R/32L and all the terminals. Therefore, NO_x contributions were higher from
 455 the south and southwest of the airport (including local on-road NO_x) compared to the those from the northeast.
 456 The lowest NO_x concentrations were measured under moderate wind speed conditions (above 4 m/s), as shown in
 457 Fig. S1. This is possibly due to atmospheric mixing and plume dilution caused by advection (Carslaw et al., 2006),
 458 given that ground-level source emissions are inversely proportional to wind speed. During this campaign, the
 459 AENA (REDAIR) station located at the airport provided measurements of sulphur dioxide (SO₂) and carbon
 460 monoxide (CO) (Fig. S1). Aviation activities have previously been reported as a significant source of gaseous and
 461 vapour-phase pollutants, such as SO₂, CO and NO_x (Masiol and Harrison, 2014). In the same vein, mobile sources,
 462 such as vehicle exhaust, generally contribute to the increase in CO and NO_x levels, as motor vehicle emissions
 463 are the dominant sources of CO and NO_x emissions in urban areas (Yu et al., 2004). Given that Barajas airport is
 464 situated near Madrid and significantly influenced by external sources, particularly traffic on the southwest side of
 465 the airport, it experiences considerable environmental impact. Therefore, the ratios of SO₂/NO_x and CO/*e*BC were
 466 used in this analysis as indicators of the relative emission strengths associated with aircraft movements. The
 467 SO₂/NO_x ratio would increase in the case of aviation emissions compared to traffic emissions, since NO_x emissions
 468 from aircraft are difficult to distinguish due to the major influence of other sources (Yu et al., 2004; Carslaw et
 469 al., 2006). Consequently, in situations where there are substantial levels of NO_x emissions, the SO₂/NO_x ratio will
 470 be low due to the impact of on-road vehicles emissions. This enables the identification of aircraft's relative
 471 contribution at the airport, as shown in Fig.9. The analysis of the SO₂/NO_x and CO/*e*BC concentration ratios at
 472 Madrid-Barajas Airport in October 2021 varies based on wind direction and speed. The bivariate polar plots shown
 473 in Fig. 9 indicate higher SO₂/NO_x and CO/*e*BC ratios were measured when dominant winds originating from the
 474 northeast of the airport, where there was minimal or no contribution from road traffic. The higher SO₂/NO_x and
 475 CO/*e*BC ratios suggest the potential impact of aircraft taxiing and taking off on local ambient SO₂ and CO
 476 concentrations, particularly when winds originate from northeast, where the 18L/36R runways are located. SO₂
 477 emissions are primarily associated with the sulphur content of the fuel and emissions from aircraft activities at the
 478 airport, such as approach, taxi-idle and climb. As a result, SO₂ plays a significant role in tracing aircraft emissions
 479 at a local scale (Yang et al., 2018). Black carbon (*e*BC) and carbon monoxide (CO) are primarily produced by

480 incomplete or inefficient combustion. Around the airport perimeter, aircraft are a significant contributor to CO
 481 emissions. Therefore, it's possible for aircraft engines to emit more CO compared to emissions from road traffic,
 482 due to the duration spent at the airport in taxiing /idling mode (Yu et al., 2004; Zhu et al., 2011). The CO/eBC
 483 ratio significantly varies with the source (Bond et al., 2004), indicating the presence of different emission sources
 484 in the vicinity of the airport, as previously reported. The highest levels of CO from aircraft are emitted at low
 485 engine power settings, such as during taxiing and idling. This significantly impacts air quality within the airport
 486 perimeter, as idle and taxi phases constitute the majority of the time an aircraft spends at the airport (Stettler et
 487 al., 2011; Yunos et al., 2017). Higher CO/eBC ratio in air parcels originating from the northeast can also be
 488 attributed to aircraft activity on runways 18L/36R, which is located northeast of the measurement station.
 489 Conversely, SO₂/NO_x and CO/eBC ratios were lower (ranging from 0 to 0.4) when winds originated from the
 490 southwest, due to significant sources of NO_x and eBC in this direction, such as nearby road traffic. Based on the
 491 polar plots shown in Fig. 9, an aircraft SO₂ and CO signal is identified to the east and northeast, distinct from the
 492 wind-dependant NO_x pattern. Further details regarding the daily variation of meteorological parameters and trace
 493 gases during the sampling period are available in the supplementary material (Fig. S1).

494



510

511 **Figure 9. Bivariate polar plots of SO₂/NO_x and CO/eBC ratios at the airport. The angular contributions of SO₂ and**
 512 **CO is different compared to the PMF determined factors. The plots indicates that the flight activities at the east and**
 513 **northeast where the 18L/36R runway is located are the source of increase in SO₂ and CO.**

514

515 4. Conclusion

516

517 This study identified the impact of an international airport on the local air quality. As part of the AVIATOR
 518 campaign, several measurements were conducted at the Madrid–Barajas Airport, in October 2021 for monitoring
 519 the chemical composition of sub-micron particles and ambient trace gas concentrations near runway. Assessing
 520 the impact of Madrid–Barajas Airport emissions on local air quality is challenging because of the complex nature
 521 of airport emissions and the strong influence from urban emissions. The proximity of the airport to urban areas,
 522 major highways, roads, and terminal buildings (T1, T2, T3, T4 and TS4) further complicates the task, making it
 523 difficult to clearly identify the specific contributions of aircraft emissions. However, aircraft emissions are
 524 characterized by high levels of unburned hydrocarbons, SO₂, CO and particulate black carbon (eBC) which are
 525 more concentrated around the airport facilities and runways. Therefore, looking at elevated levels of these markers
 526 might indicate a stronger influence from aviation-related activities, especially during times of high airport traffic.
 527 Total non-refractory particles were dominated by organics (more than 72% of the total). Sulphate particles were
 528 the second most abundant chemical species and accounted for about 13% of the total aerosol. Based on AMS data
 529 (Ratio of *m/z* 85:71), no significant oil fraction in the organic particulate matter (PM) samples were measured.
 530 This could indicate the absence of oil in sub-micron particle size range or due to the method used in this study
 531 (AMS) is not able to identify lubricant oil in PM. Thus, further measurements with improved measurement
 532 technique may be required to identify oil fraction in sub-micron organic aerosol. Trace gases were also monitored
 533 along with the particle monitoring tools. Average ambient concentrations of eBC, NO_x, SO₂, PM_{2.5}, PM₁₀ at the
 534 airport during October 2021 were 1.07, 22.7, 4.10, 9.35, and 16.43 (µg/m³), respectively. NO_x contribution at the
 535 sampling point was highest when the winds originating from south and southeast of the airport. There are two
 536 motorways with road traffic are located at the same direction as well as terminal buildings and southern runways.
 537 Therefore, NO_x concentrations were more likely determined by on-road traffic compared to the aircraft activity at
 538 the sampling point. Sources of organic aerosols (as the most abundant non-refractory aerosol group) were
 539 identified using Positive Matrix Factorisation (PMF) analysis. PMF was able to discriminate three main significant
 540 sources: Less Oxidised Oxygenated Organic Aerosol (LO-OOA), Alkane Organic Aerosol (AlkOA), and More
 541 Oxidised Oxygenated Organic Aerosol (MO OOA). The sum of LO-OOA and MO OOA fractions accounting for
 542 more than 80% of the total organic mass throughout the campaign, LO-OOA had the highest relative intensity

543 (RI) at m/z 43 (which is characteristic of LO-OOA), MO-OOA had a high RI at m/z 28 and 44 these indicate a
544 potential secondary aerosol fraction. Third factor, AlkOA, had high RIs at m/z 43, 57 and 85 (attributed to decane
545 previously) which is related to jet fuel vapour (Smith et al., 2022). Bivariate polar plots were used to angular PMF
546 determined factor and ambient trace gas distributions based on wind speed and wind direction at the airport. It has
547 been found that, the PMF determined factors had highest relative contributions when the winds originating from
548 the west and southwest of the airport where runways 14R/32L and 18R/36L, as well as terminals T1, T2, T3, T4
549 and TS4, are located. The SO_2/NO_x and $\text{CO}/e\text{BC}$ ratio have been shown to represent a useful tool for assessing
550 relative emission strength associated with aircraft movements. Take-off activities at the northeast of the
551 measurement station were identified as a potential local source of SO_2 and CO in Barajas-Madrid. Angular
552 correlation analysis based on wind direction and speed indicated that $e\text{BC}$ and THC emissions are potentially
553 determined by aircraft take off activities at 18L/36R runway located along the east and northeast of the sampling
554 point where more than 50% of the take-off activity took place in the sampling period.
555 There are two previously reported significant ways to reduce aviation emissions at airports, improving efficiency
556 of the processes emitting air pollutants such as electrification of airport taxiway operations (Salihu et al., 2021),
557 and switching to sustainable alternative fuels where applicable. Improved ground activities at airports such as
558 electric aircraft towing system can potentially lead up to 82 % reduction in CO_2 emissions (van Baaren, 2019),
559 while switching to SAF alone reduce Landing-takeoff cycle (LTO) emissions up to 70 % compared to fossil fuel
560 (Schripp et al., 2022). Further, SAF use for auxiliary power units (APU) also potentially reduce NO_x and CO_2
561 emissions by at least 5%. Therefore, improving energy efficiency of ground activities at airports and using SAF
562 are recommended for policymakers to improve the overall air quality at airports.

563

564 *Author contributions.* **Saleh Alzahrani, Doğuşhan Kılıç, Michael Flynn, Paul I. Williams and James Allan**
565 designed the project; **Saleh Alzahrani, Doğuşhan Kılıç, Michael Flynn and Paul I. Williams** performed the
566 fieldwork; **Saleh Alzahrani** performed the data analysis, and wrote – original draft of the article; **Doğuşhan**
567 **Kılıç** reviewed and edited the article; **Paul I. Williams and James Allan** supervised, reviewed and edited the
568 article.

569

570 *Competing interests.* At least one of the (co-) authors is a member of the editorial board of Atmospheric
571 Chemistry and Physics.

572

573 **Acknowledgments**

574

575 This project has received funding from the European Union’s Horizon 2020 research and innovation programme
576 under Grant Agreement No 814801.

577

578 **References**

579

580 Air transport statistics: europa.eu, 2022.

581

582 Alfarra, M.R., Prevot, A.S., Szidat, S., Sandradewi, J., Weimer, S., Lanz, V.A., Schreiber, D., Mohr, M. and
583 Baltensperger, U.: Identification of the mass spectral signature of organic aerosols from wood burning
584 emissions. *Environmental science & technology*, 41(16), pp.5770-5777, 2007.

585

586 Amato, F., Moreno, T., Pandolfi, M., Querol, X., Alastuey, A., Delgado, A., Pedrero, M. and Cots, N.:
587 Concentrations, sources and geochemistry of airborne particulate matter at a major European airport. *Journal of*
588 *Environmental Monitoring*, 12(4), pp.854-862, <https://doi.org/10.1039/B925439K>, 2010.

589

590 Anderson, B.E., Beyersdorf, A.J., Hudgins, C.H., Plant, J.V., Thornhill, K.L., Winstead, E.L., Ziemba, L.D.,
591 Howard, R., Corporan, E., Miake-Lye, R.C. and Herndon, S.C.: Alternative aviation fuel experiment
592 (AAFEX) (No. NASA/TM-2011-217059), 2011.

593

594 Anderson, B.E., Chen, G. and Blake, D.R.: Hydrocarbon emissions from a modern commercial
595 airliner. *Atmospheric Environment*, 40(19), pp.3601-3612, <https://doi.org/10.1016/j.atmosenv.2005.09.072>,
596 2006.

597

598 Bond, T.C., Streets, D.G., Yarber, K.F., Nelson, S.M., Woo, J.H. and Klimont, Z.: A technology-based global
599 inventory of black and organic carbon emissions from combustion. *Journal of Geophysical Research:*
600 *Atmospheres*, 109(D14), <https://doi.org/10.1029/2003JD003697>, 2004.

601

602 Boldo, E., Medina, S., Le Tertre, A., Hurley, F., Mücke, H.G., Ballester, F., Aguilera, I. and Daniel Eilstein on
603 behalf of the Apehis group.: Apehis: Health impact assessment of long-term exposure to PM 2.5 in 23 European
604 cities. *European journal of epidemiology*, 21, pp.449-458, <https://doi.org/10.1007/s10654-006-9014-0>, 2006.
605

606 Canagaratna, M.R., Jayne, J.T., Jimenez, J.L., Allan, J.D., Alfarra, M.R., Zhang, Q., Onasch, T.B., Drewnick,
607 F., Coe, H., Middlebrook, A. and Delia, A.: Chemical and microphysical characterization of ambient aerosols
608 with the aerodyne aerosol mass spectrometer. *Mass spectrometry reviews*, 26(2), pp.185-222,
609 <https://doi.org/10.1002/mas.20115>, 2007.
610

611 Canonaco, F., Crippa, M., Slowik, J.G., Baltensperger, U. and Prévôt, A.S.: SoFi, an IGOR-based interface for
612 the efficient use of the generalized multilinear engine (ME-2) for the source apportionment: ME-2 application to
613 aerosol mass spectrometer data. *Atmospheric Measurement Techniques*, 6(12), pp.3649-3661,
614 <https://doi.org/10.5194/amt-6-3649-2013>, 2013.
615

616 Carslaw, D.C., Beevers, S.D., Ropkins, K. and Bell, M.C.: Detecting and quantifying aircraft and other on-
617 airport contributions to ambient nitrogen oxides in the vicinity of a large international airport. *Atmospheric
618 Environment*, 40(28), pp.5424-5434, <https://doi.org/10.1016/j.atmosenv.2006.04.062>, 2006.
619

620 Carslaw, D.C. and Ropkins, K.: Openair—an R package for air quality data analysis. *Environmental Modelling
621 & Software*, 27, pp.52-61, <https://doi.org/10.1016/j.envsoft.2011.09.008> , 2012.
622

623 Crilley, L.R., Bloss, W.J., Yin, J., Beddows, D.C., Harrison, R.M., Allan, J.D., Young, D.E., Flynn, M.,
624 Williams, P., Zotter, P. and Prévôt, A.S.: Sources and contributions of wood smoke during winter in London:
625 assessing local and regional influences. *Atmospheric chemistry and physics*, 15(6), pp.3149-3171,
626 <https://doi.org/10.5194/acp-15-3149-2015>, 2015.
627

628 Environmental protection. Annex 16 to the Convention on International Civil Aviation. Volume II aircraft
629 engine emissions. I.C.A.O., 2016.
630

631 Fushimi, A., Saitoh, K., Fujitani, Y. and Takegawa, N.: Identification of jet lubrication oil as a major component
632 of aircraft exhaust nanoparticles. *Atmospheric Chemistry and Physics*, 19(9), pp.6389-6399, 2019.
633

634 He, R.W., Shirmohammadi, F., Gerlofs-Nijland, M.E., Sioutas, C. and Cassee, F.R.: Pro-inflammatory
635 responses to PM_{0.25} from airport and urban traffic emissions. *Science of the total environment*, 640, pp.997-
636 1003, <https://doi.org/10.1016/j.scitotenv.2018.05.382>, 2018.
637

638 Herndon, S.C., Jayne, J.T., Lobo, P., Onasch, T.B., Fleming, G., Hagen, D.E., Whitefield, P.D. and Miake-Lye,
639 R.C.: Commercial aircraft engine emissions characterization of in-use aircraft at Hartsfield-Jackson Atlanta
640 International Airport. *Environmental science & technology*, 42(6), pp.1877-1883,
641 <https://doi.org/10.1021/es072029+>, 2008.
642

643 Helin, A., Niemi, J.V., Virkkula, A., Pirjola, L., Teinilä, K., Backman, J., Aurela, M., Saarikoski, S., Rönkkö,
644 T., Asmi, E. and Timonen, H.: Characteristics and source apportionment of black carbon in the Helsinki
645 metropolitan area, Finland. *Atmospheric Environment*, 190, pp.87-98,
646 <https://doi.org/10.1016/j.atmosenv.2018.07.022>, 2018.
647

648 Hu, S., Fruin, S., Kozawa, K., Mara, S., Winer, A.M. and Paulson, S.E.: Aircraft emission impacts in a
649 neighborhood adjacent to a general aviation airport in Southern California. *Environmental science &
650 technology*, 43(21), pp.8039-8045, <https://doi.org/10.1021/es900975f>, 2009.
651

652 Hudda, N. and Fruin, S.A.: International airport impacts to air quality: size and related properties of large
653 increases in ultrafine particle number concentrations. *Environmental science & technology*, 50(7), pp.3362-
654 3370, <https://doi.org/10.1021/acs.est.5b05313>, 2016.
655

656 Hudda, N., Gould, T., Hartin, K., Larson, T.V. and Fruin, S.A.: Emissions from an international airport increase
657 particle number concentrations 4-fold at 10 km downwind. *Environmental science & technology*, 48(12),
658 pp.6628-6635, <https://doi.org/10.1021/es5001566>, 2014.
659

660 Hudda, N., Simon, M.C., Zamore, W., Brugge, D. and Durant, J.L.: Aviation emissions impact ambient ultrafine
661 particle concentrations in the greater Boston area. *Environmental science & technology*, 50(16), pp.8514-8521,
662 <https://doi.org/10.1021/acs.est.6b01815>, 2016.

663
664 Jimenez, J.L., Canagaratna, M.R., Donahue, N.M., Prevot, A.S.H., Zhang, Q., Kroll, J.H., DeCarlo, P.F., Allan,
665 J.D., Coe, H., Ng, N.L. and Aiken, A.C.: Evolution of organic aerosols in the atmosphere. *Science*, 326(5959),
666 pp.1525-1529, <https://doi.org/10.1126/science.118035>, 2009.

667
668 Jonsdottir, H.R., Delaval, M., Leni, Z., Keller, A., Brem, B.T., Siegerist, F., Schönenberger, D., Durdina, L.,
669 Elser, M., Burtscher, H. and Liati, A.: Non-volatile particle emissions from aircraft turbine engines at ground-
670 idle induce oxidative stress in bronchial cells. *Communications biology*, 2(1), p.90,
671 <https://doi.org/10.1038/s42003-019-0332-7>, 2019.

672
673 Kinsey, J.S.: Characterization of emissions from commercial aircraft engines during the Aircraft Particle
674 Emissions eXperiment (APEX) 1 to 3. Office of Research and Development, US Environmental Protection
675 Agency, 2009.

676
677 Kinsey, J.S., Dong, Y., Williams, D.C. and Logan, R.: Physical characterization of the fine particle emissions
678 from commercial aircraft engines during the Aircraft Particle Emissions eXperiment (APEX) 1–3. *Atmospheric
679 Environment*, 44(17), pp.2147-2156, <https://doi.org/10.1016/j.atmosenv.2010.02.010>, 2010.

680
681 Kinsey, J.S., Hays, M.D., Dong, Y., Williams, D.C. and Logan, R.: Chemical characterization of the fine
682 particle emissions from commercial aircraft engines during the Aircraft Particle Emissions eXperiment (APEX)
683 1 to 3. *Environmental science & technology*, 45(8), pp.3415-3421, <https://doi.org/10.1021/es103880d>, 2011.

684
685 Lee, D.S., Pitari, G., Grewe, V., Gierens, K., Penner, J.E., Petzold, A., Prather, M.J., Schumann, U., Bais, A.,
686 Berntsen, T. and Iachetti, D.: Transport impacts on atmosphere and climate: Aviation. *Atmospheric
687 environment*, 44(37), pp.4678-4734, <https://doi.org/10.1016/j.atmosenv.2009.06.005>, 2010.

688
689 Li, N., Hao, M., Phalen, R.F., Hinds, W.C. and Nel, A.E.: Particulate air pollutants and asthma: a paradigm for
690 the role of oxidative stress in PM-induced adverse health effects. *Clinical immunology*, 109(3), pp.250-265,
691 <https://doi.org/10.1016/j.clim.2003.08.006>, 2003.

692
693 Liu, G., Yan, B. and Chen, G.: Technical review on jet fuel production. *Renewable and Sustainable Energy
Reviews*, 25, pp.59-70, 2013.

694
695 Masiol, M. and Harrison, R.M.: Aircraft engine exhaust emissions and other airport-related contributions to
696 ambient air pollution: A review. *Atmospheric Environment*, 95, pp.409-455,
697 <https://doi.org/10.1016/j.atmosenv.2014.05.070>, 2014.

698
699 Mazaheri, M., Johnson, G.R. and Morawska, L.: An inventory of particle and gaseous emissions from large
700 aircraft thrust engine operations at an airport. *Atmospheric Environment*, 45(20), pp.3500-3507,
701 <https://doi.org/10.1016/j.atmosenv.2010.12.012>, 2011.

702
703 NIST Mass Spectrometry Data Center. Decane, US secretary of commerce.
704 <https://webbook.nist.gov/cgi/cbook.cgi?ID=C124185&Mask=200#Mass-Spec>, 1990.

705
706 Onasch, T.B., Jayne, J.T., Herndon, S., Worsnop, D.R., Miake-Lye, R.C., Mortimer, I.P. and Anderson, B.E.:
707 Chemical properties of aircraft engine particulate exhaust emissions. *Journal of Propulsion and Power*, 25(5),
pp.1121-1137, <https://doi.org/10.2514/1.36371>, 2009.

708
709 Paatero, P.: The multilinear engine—a table-driven, least squares program for solving multilinear problems,
710 including the n-way parallel factor analysis model. *Journal of Computational and Graphical Statistics*, 8(4),
pp.854-888, <https://doi.org/10.1080/10618600.1999.10474853>, 1999.

711
712 Paatero, P. and Tapper, U.: Positive matrix factorization: A non-negative factor model with optimal utilization
713 of error estimates of data values. *Environmetrics*, 5(2), pp.111-126, <https://doi.org/10.1002/env.3170050203>,
714 1994.

715 Petzold, A. and Schönlinner, M.: Multi-angle absorption photometry—a new method for the measurement of
716 aerosol light absorption and atmospheric black carbon. *Journal of Aerosol Science*, 35(4), pp.421-441,
717 <https://doi.org/10.1016/j.jaerosci.2003.09.005>, 2004.

718 Pope III, C.A. and Dockery, D.W.: Health effects of fine particulate air pollution: lines that connect. *Journal of*
719 *the air & waste management association*, 56(6), pp.709-742, <https://doi.org/10.1080/10473289.2006.10464485>,
720 2006.

721 Reyes-Villegas, E., Green, D.C., Priestman, M., Canonaco, F., Coe, H., Prévôt, A.S. and Allan, J.D.: Organic
722 aerosol source apportionment in London 2013 with ME-2: exploring the solution space with annual and seasonal
723 analysis. *Atmospheric Chemistry and Physics*, 16(24), pp.15545-15559, [https://doi.org/10.5194/acp-16-15545-](https://doi.org/10.5194/acp-16-15545-2016)
724 2016, 2016.

725
726 Reyes-Villegas, E., Priestley, M., Ting, Y.C., Haslett, S., Bannan, T., Le Breton, M., Williams, P.I., Bacak, A.,
727 Flynn, M.J., Coe, H. and Percival, C.: Simultaneous aerosol mass spectrometry and chemical ionisation mass
728 spectrometry measurements during a biomass burning event in the UK: insights into nitrate
729 chemistry. *Atmospheric Chemistry and Physics*, 18(6), pp.4093-4111, [https://doi.org/10.5194/acp-18-4093-](https://doi.org/10.5194/acp-18-4093-2018)
730 2018, 2018.

731
732 Rissman, J., Arunachalam, S., Woody, M., West, J.J., BenDor, T. and Binkowski, F.S.: A plume-in-grid
733 approach to characterize air quality impacts of aircraft emissions at the Hartsfield–Jackson Atlanta International
734 Airport. *Atmospheric Chemistry and Physics*, 13(18), pp.9285-9302, <https://doi.org/10.5194/acp-13-9285-2013>,
735 2013.

736
737 Salihu, A.L., Lloyd, S.M. and Ak Gunduz, A.: Electrification of airport taxiway operations: A simulation
738 framework for analyzing congestion and cost. *Transportation Research Part D: Transport and Environment*, 97,
739 p.102962, <https://doi.org/10.1016/j.trd.2021.102962>, 2021.

740
741 Schripp, T., Anderson, B.E., Bauder, U., Rauch, B., Corbin, J.C., Smallwood, G.J., Lobo, P., Crosbie, E.C.,
742 Shook, M.A., Miake-Lye, R.C. and Yu, Z.: Aircraft engine particulate matter emissions from sustainable
743 aviation fuels: Results from ground-based measurements during the NASA/DLR campaign ECLIF2/ND-
744 MAX. *Fuel*, 325, p.124764, <https://doi.org/10.1016/j.fuel.2022.124764>, 2022.

745
746 Schwarze, P.E., Øvrevik, J., Låg, M., Refsnes, M., Nafstad, P., Hetland, R.B. and Dybing, E.: Particulate matter
747 properties and health effects: consistency of epidemiological and toxicological studies. *Human & experimental*
748 *toxicology*, 25(10), pp.559-579, <https://doi.org/10.1177/096032706072520>, 2006.

749
750 Smith, L.D., Allan, J., Coe, H., Reyes-Villegas, E., Johnson, M.P., Crayford, A., Durand, E. and Williams, P.I.:
751 Examining chemical composition of gas turbine-emitted organic aerosol using positive matrix factorisation
752 (PMF). *Journal of Aerosol Science*, 159, p.105869, <https://doi.org/10.1016/j.jaerosci.2021.105869>, 2022.

753
754 Stettler, M.E.J., Eastham, S. and Barrett, S.R.H.: Air quality and public health impacts of UK airports. Part I:
755 Emissions. *Atmospheric environment*, 45(31), pp.5415-5424, <https://doi.org/10.1016/j.atmosenv.2011.07.012>,
756 2011.

757
758 Timko, M.T., Albo, S.E., Onasch, T.B., Fortner, E.C., Yu, Z., Miake-Lye, R.C., Canagaratna, M.R., Ng, N.L.
759 and Worsnop, D.R.: Composition and sources of the organic particle emissions from aircraft engines. *Aerosol*
760 *Science and Technology*, 48(1), pp.61-73, <https://doi.org/10.1080/02786826.2013.857758>, 2014.

761
762 Timko, M.T., Onasch, T.B., Northway, M.J., Jayne, J.T., Canagaratna, M.R., Herndon, S.C., Wood, E.C.,
763 Miake-Lye, R.C. and Knighton, W.B.: Gas turbine engine emissions—Part II: chemical properties of particulate
764 matter. <https://doi.org/10.1115/1.4000132>, 2010.

765
766 Ulbrich, I.M., Canagaratna, M.R., Zhang, Q., Worsnop, D.R. and Jimenez, J.L.: Interpretation of organic
767 components from Positive Matrix Factorization of aerosol mass spectrometric data. *Atmospheric Chemistry and*
768 *Physics*, 9(9), pp.2891-2918, <https://doi.org/10.5194/acp-9-2891-2009>, 2009.

769
770 Ungeheuer, F., Caudillo, L., Ditas, F., Simon, M., van Pinxteren, D., Kılıç, D., Rose, D., Jacobi, S., Kürten, A.,
771 Curtius, J. and Vogel, A.L.: Nucleation of jet engine oil vapours is a large source of aviation-related ultrafine

772 particles. *Communications Earth & Environment*, 3(1), p.319, <https://doi.org/10.1038/s43247-022-00653-w>,
773 2022.
774
775 van Baaren, E.: The feasibility of a fully electric aircraft towing system. 2019.
776
777 Westerdahl, D., Fruin, S.A., Fine, P.L. and Sioutas, C.: The Los Angeles International Airport as a source of
778 ultrafine particles and other pollutants to nearby communities. *Atmospheric Environment*, 42(13), pp.3143-
779 3155, <https://doi.org/10.1016/j.atmosenv.2007.09.006>, 2008.
780
781 Yang, X., Cheng, S., Lang, J., Xu, R. and Lv, Z.: Characterization of aircraft emissions and air quality impacts
782 of an international airport. *Journal of environmental sciences*, 72, pp.198-207,
783 <https://doi.org/10.1016/j.jes.2018.01.007>, 2018.
784
785 Yim, S.H., Stettler, M.E. and Barrett, S.R.: Air quality and public health impacts of UK airports. Part II: Impacts
786 and policy assessment. *Atmospheric environment*, 67, pp.184-192,
787 <https://doi.org/10.1016/j.atmosenv.2012.10.017>, 2013.
788
789 Yu, K.N., Cheung, Y.P., Cheung, T. and Henry, R.C.: Identifying the impact of large urban airports on local air
790 quality by nonparametric regression. *Atmospheric Environment*, 38(27), pp.4501-4507,
791 <https://doi.org/10.1016/j.atmosenv.2004.05.034>, 2004.
792
793 Yu, Z., Herndon, S.C., Ziemba, L.D., Timko, M.T., Liscinsky, D.S., Anderson, B.E. and Miake-Lye, R.C.:
794 Identification of lubrication oil in the particulate matter emissions from engine exhaust of in-service commercial
795 aircraft. *Environmental science & technology*, 46(17), pp.9630-9637, <https://doi.org/10.1021/es301692t>, 2012.
796
797 Yu, Z., Liscinsky, D.S., Winstead, E.L., True, B.S., Timko, M.T., Bhargava, A., Herndon, S.C., Miake-Lye,
798 R.C. and Anderson, B.E.: Characterization of lubrication oil emissions from aircraft engines. *Environmental*
799 *science & technology*, 44(24), pp.9530-9534, <https://doi.org/10.1021/es102145z>, 2010.
800
801 Yu, Z., Timko, M.T., Herndon, S.C., Richard, C., Beyersdorf, A.J., Ziemba, L.D., Winstead, E.L. and Anderson,
802 B.E.: Mode-specific, semi-volatile chemical composition of particulate matter emissions from a commercial gas
803 turbine aircraft engine. *Atmospheric Environment*, 218, p.116974,
804 <https://doi.org/10.1016/j.atmosenv.2019.116974>, 2019.
805
806 Yunos, S.N.M.M., Ghafir, M.F.A. and Wahab, A.A.: April. Aircraft LTO emissions regulations and
807 implementations at European airports. In *AIP Conference Proceedings* (Vol. 1831, No. 1),
808 <https://doi.org/10.1063/1.4981147>, 2017.
809
810 Zhang, Q., Jimenez, J.L., Canagaratna, M.R., Allan, J.D., Coe, H., Ulbrich, I., Alfarra, M.R., Takami, A.,
811 Middlebrook, A.M., Sun, Y.L. and Dzepina, K.: Ubiquity and dominance of oxygenated species in organic
812 aerosols in anthropogenically-influenced Northern Hemisphere midlatitudes. *Geophysical research*
813 *letters*, 34(13), <https://doi.org/10.1029/2007GL029979>, 2007.
814
815 Zhu, Y., Fanning, E., Yu, R.C., Zhang, Q. and Froines, J.R.: Aircraft emissions and local air quality impacts
816 from takeoff activities at a large International Airport. *Atmospheric Environment*, 45(36), pp.6526-6533,
817 <https://doi.org/10.1016/j.atmosenv.2011.08.062>, 2011.
818
819
820
821
822
823